

Electronic Supplement Information of

Effect of Aging Conditions at Equal OH Exposure in an Oxidation Flow Reactor on the Composition of Toluene-derived Secondary Organic Aerosol

Hendryk Czech^{1,2,3,*}, Pasi Yli-Pirilä², Petri Tiitta^{2,a}, Mika Ihälainen², Anni Hartikainen², Eric Schneider^{1,4}, Patrick Martens^{1,b}, Andreas Paul^{1,5}, Thorsten Hohaus⁵, Christopher P. Rüger^{1,4}, Jorma Jokiniemi², Ralf Zimmermann^{1,3,4}, Olli Sippula^{2,6}

¹Chair of Analytical Chemistry, University of Rostock, 18059, Rostock, Germany

²Fine Particle and Aerosol Technology Laboratory, Department of Environmental and Biological Science, University of Eastern Finland, 70211, Kuopio, Finland

³Cooperation Group “Comprehensive Molecular Analytics” (CMA), Helmholtz Zentrum München, 81379, München, Germany

⁴Department “Life, Light and Matter”, University of Rostock, 18059, Rostock, Germany

⁵Institute of Energy and Climate Research: Troposphere (IEK-8), Forschungszentrum Jülich, 52425, Jülich, Germany

⁶Department of Chemistry, University of Eastern Finland, 80101, Joensuu, Finland

^anow at: Envineer Oy, Kuopio, Finland

^bnow at: Desert Research Institute (DRI), Reno, NV, USA

*corresponding author: hendryk.czech@uni-rostock.de

Table of Content

Table S1	RO ₂ fate
Table S2	LVOC fate with full tol-SOA size distribution
Table S3	LVOC fate with half tol-SOA size distribution
Table S4	tol-SOA bulk composition from AMS
Figure S1	Particle number size distribution (SMPS)
Figure S2	Distribution of carbon fractions (TOCA)
Figure S3	Eigenvalues of principal components
Figure S4	ESI(\pm) average mass spectra
Figure S5	#C vs. OS _C from ESI- mass spectra
Figure S6	Venn diagram

Table S1. RO₂ fate for “low”, “medium” and “high” OFR254 conditions resembling “safer”, “transition” and “riskier” OFR condition.

experiment	OH	HO ₂	RO ₂	Isomerization
low1	56.3 %	43.6 %	0	0.1 %
low2	56.3 %	43.6 %	0	0.1 %
low3	56.3 %	43.6 %	0	0.1 %
medium1	67.4 %	32.5 %	0	0
medium2	67.4 %	32.5 %	0	0
medium3	67.4 %	32.5 %	0	0
high1	87.9 %	12.0 %	0.1 %	0
high2	87.9 %	12.0 %	0.1 %	0
high3	87.9 %	12.0 %	0.1 %	0

Table S2. Fraction (F) of the LVOC fate divided to condensation on particles (F_{par}), further oxidation by OH (F_{OH}), loss to the inner wall (F_{wall}) or exiting OFR in gas phase (F_{exit}) using the particle number concentration after the PEAR.

experiment	F _{par}	F _{OH}	F _{wall}	F _{exit}
low1	91.1 %	4.6 %	2.7 %	1.5 %
low2	90.9 %	4.9 %	2.7 %	1.5 %
low3	84.0 %	7.3 %	3.7 %	5.0 %
medium1	96.6 %	2.2 %	1.2 %	0.0 %
medium2	95.6 %	2.9 %	1.5 %	0.1 %
medium3	94.3 %	3.7 %	1.8 %	0.2 %
high1	99.4 %	0.4 %	0.2 %	0.0 %
high2	99.3 %	0.4 %	0.2 %	0.0 %
high3	99.2 %	0.6 %	0.3 %	0.0 %

Table S3. Same as Table S3 but using half of the particle number concentration after the PEAR.

experiment	F _{par}	F _{OH}	F _{wall}	F _{exit}
Low1	77.2 %	7.9 %	4.6 %	10.4 %
Low2	76.7 %	8.3 %	4.6 %	10.4 %
Low3	64.4 %	11.2 %	5.6 %	18.7 %
Medium1	92.7 %	4.3 %	2.3 %	0.7 %
Medium2	89.9 %	5.4 %	2.8 %	1.9 %
Medium3	86.3 %	6.7 %	3.3 %	3.6 %
High1	98.7 %	0.8 %	0.4 %	0.0 %
High2	98.6 %	0.9 %	0.5 %	0.0 %
High3	98.3 %	1.1 %	0.6 %	0.0 %

Table S4. Elemental bulk aerosol composition (H:C and O:C), molar ratio of organic matter to organic carbon (OM:OC) and average carbon oxidation state (OS_c) from aerosol mass spectrometry (AMS). “x” indicate significant differences between types of tol-SOA after one-way ANOVA posthoc multiple comparisons corrected by Bonferroni method at a significance level of 0.05.

	O:C	H:C	OM:OC	OS_c
low1	0.95	1.64	2.41	0.25
low2	0.94	1.65	2.39	0.23
low3	0.96	1.64	2.41	0.27
med1	0.92	1.65	2.36	0.18
med2	0.92	1.66	2.37	0.18
med3	0.93	1.65	2.38	0.20
high1	0.80	1.64	2.20	-0.05
high2	0.79	1.64	2.19	-0.07
high3	0.79	1.65	2.19	-0.07
cham1	0.87	1.48	2.28	0.26
cham2	0.85	1.48	2.26	0.23
cham3	0.85	1.47	2.26	0.23
low vs. medium	x	x	x	x
low vs. high	x	x	x	x
low vs. cham	x	x	x	x
medium vs.-high	x		x	x
medium-vs. cham	x		x	x
high vs. cham	x		x	

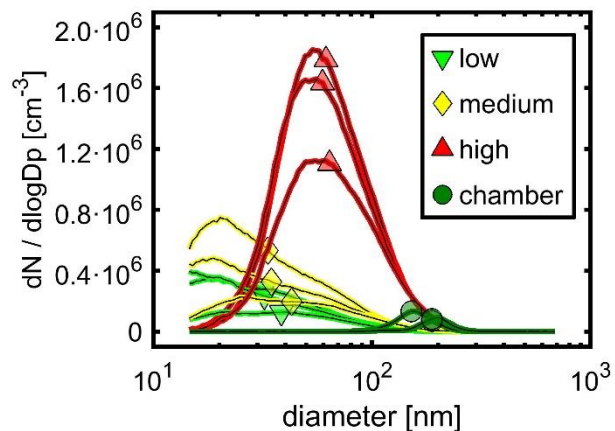


Fig. S1 Size distribution of tol-SOA based on particle number concentration, derived from SMPS. Symbols indicate geometric mean particle diameter.

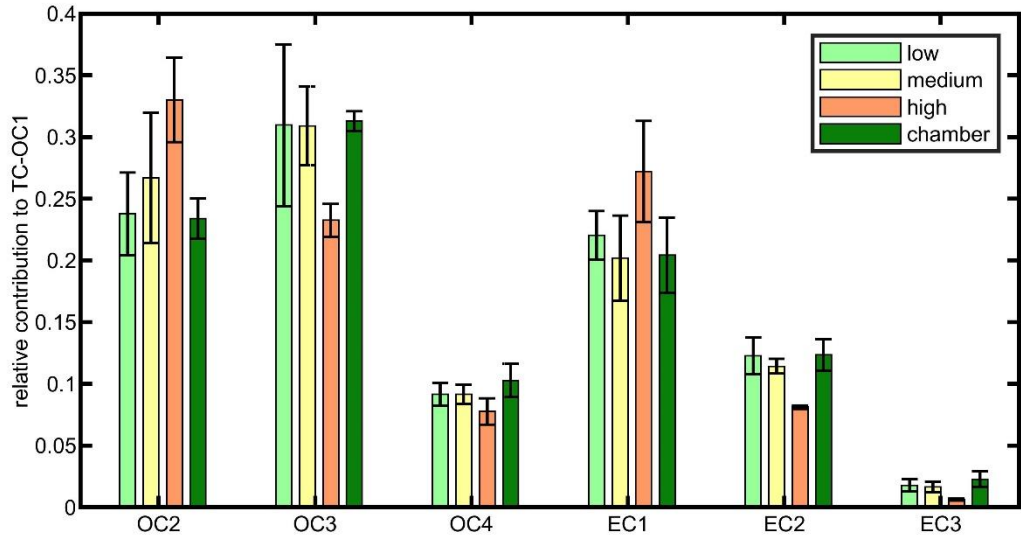


Fig. S2 Distribution of individual carbon fraction according to *Improve_A* protocol. OC1 was discarded from the total carbon (TC) because of likely blow-off by different sampling durations. Error bars refer to standard deviation (s.d.) and each group contains three replicates (n=3).

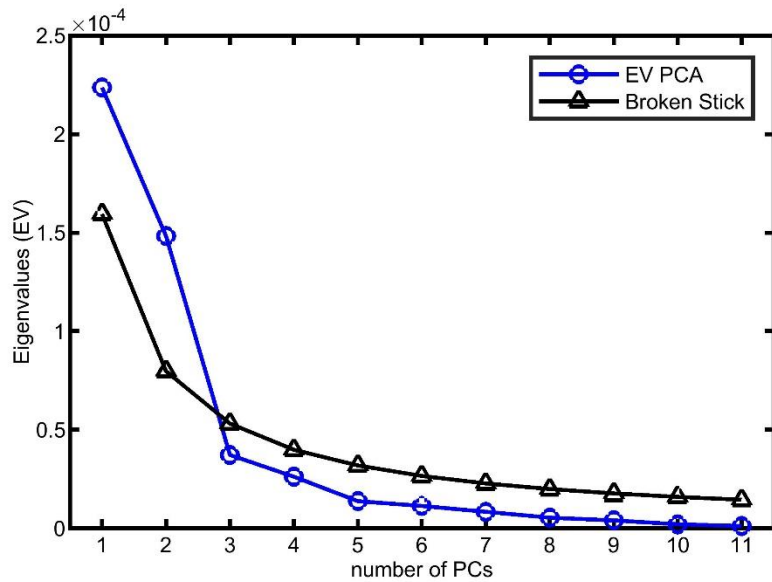


Fig. S3 Determination of number of PCs by “broken stick” approach.

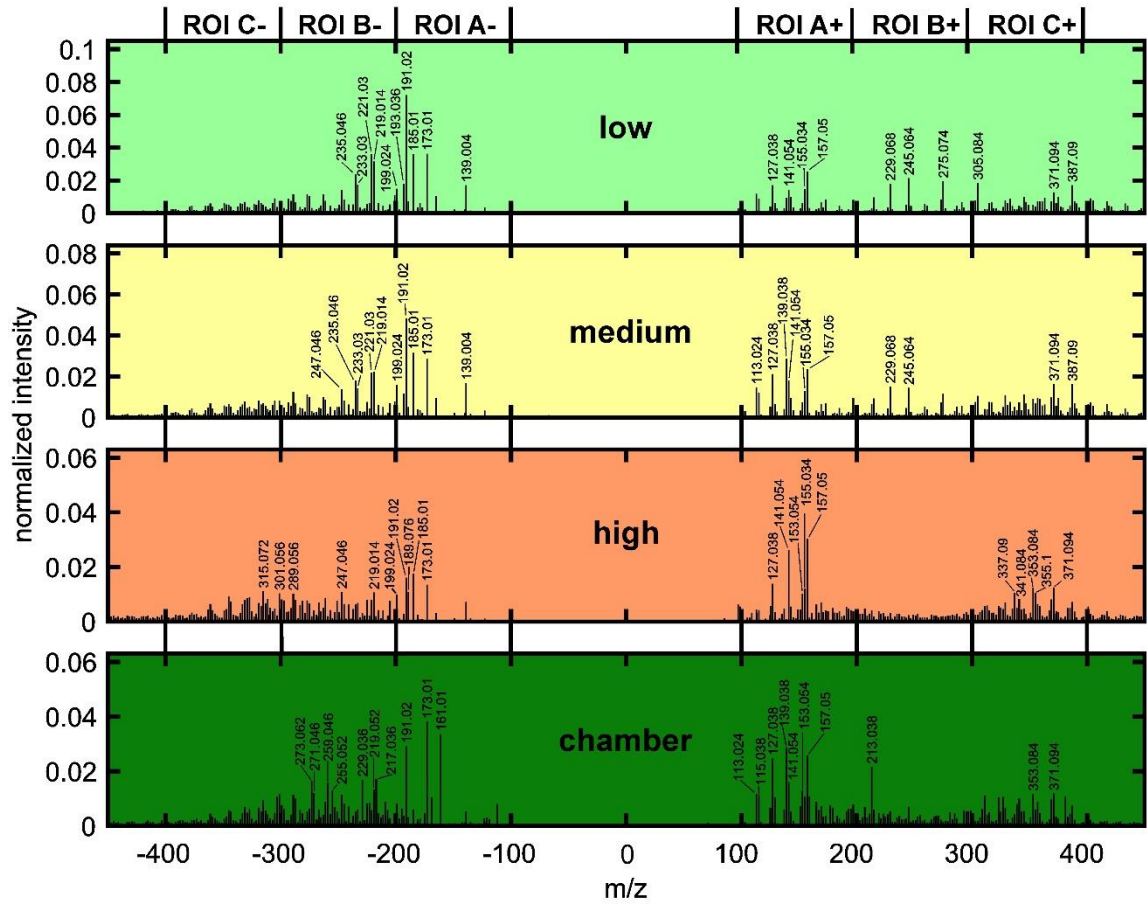


Fig. S4 Mean mass spectra of four tol-SOA types with top 10 m/z labelled by exact mass. Complete m/z range is reduced to ± 450 . m/z ranges of regions of interests (ROI) are indicated from A to C for ESI(\pm).

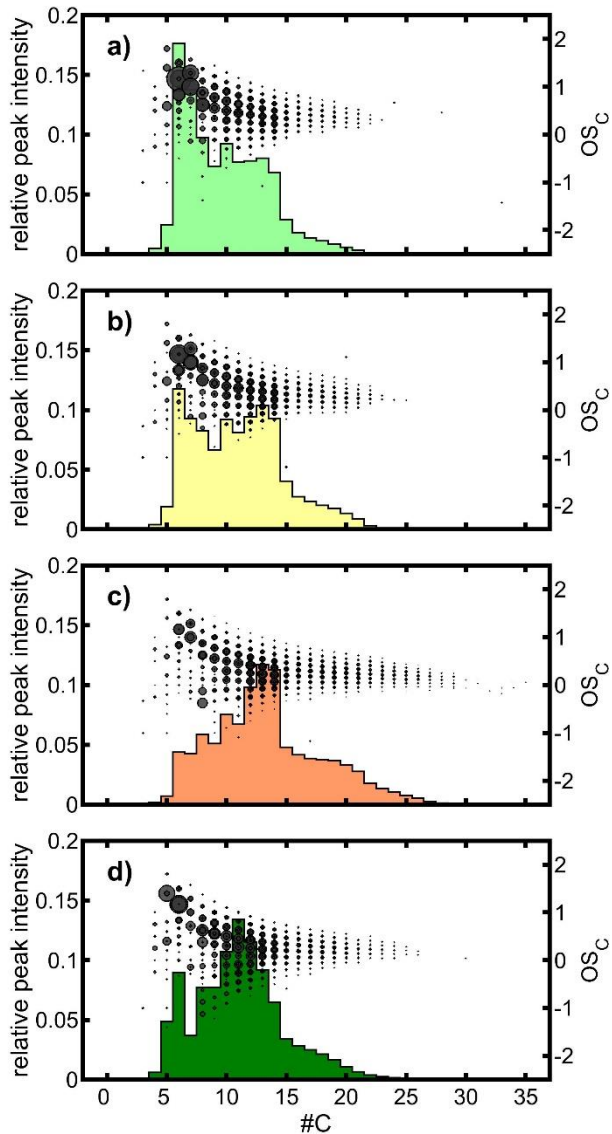


Fig. S5 #C vs. OSC with summed relative intensities for each #C for ESI(-) of a) “low”, b) “medium”, c) “high” and d) “cham”.

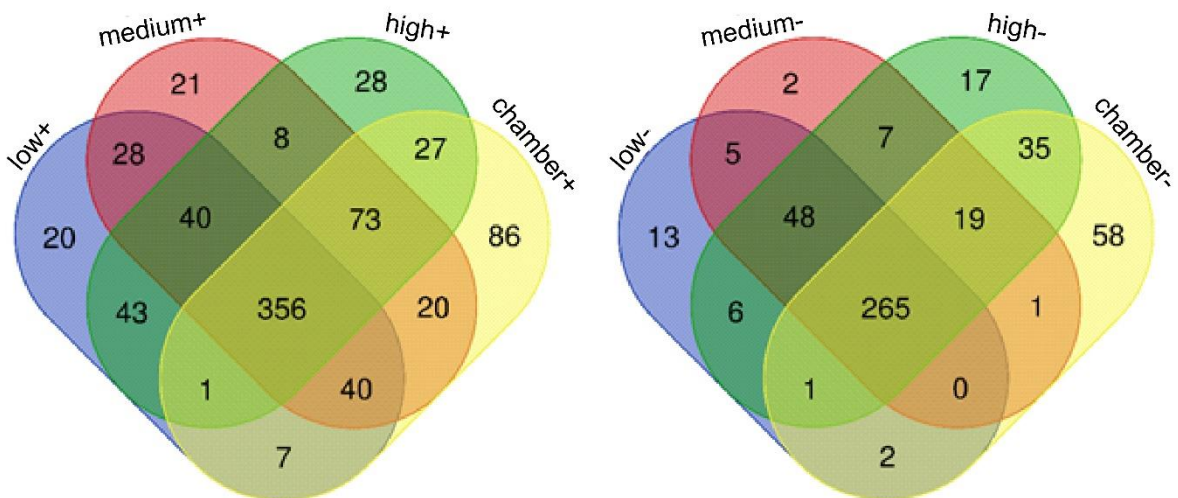


Fig. S6 Venn diagram with sum formula with $\#C \leq 15$ from ESI(+) (left) and ESI(-) (right).